European Journal of Medicinal Chemistry 46 (2011) 1117–1121

Contents lists available at ScienceDirect

European Journal of Medicinal Chemistry

journal homepage: http://www.elsevier.com/locate/ejmech

Original article

Identification, structural properties and chelating capacity of miltipolone as a broad-spectrum inhibitor to cancer cells

Jing Wang [a], Shaopeng Chen [b], Hao Cheng [b], Fangyi Yang [b], Junting Wan [b], Jian Bo [b,1], Yingxue Liu [b], Junyun Yang [b], Jinsong Liu [b], Guo-Chun Zhou [c,d,*]

[a] Department of Applied Chemistry, College of Sciences, Nanjing Agricultural University, Nanjing, Jiangsu 210095, PR China
[b] Guangzhou Institute of Biomedicine and Health, Chinese Academy of Sciences, Guangzhou, Guangdong 510530, PR China
[c] College of Biotechnology and Pharmaceutical Engineering, Nanjing University of Technology, Nanjing 210009, PR China
[d] College of Pharmaceutical Sciences, Nanjing University of Technology, Nanjing 210009, PR China

ARTICLE INFO

Article history:
Received 30 October 2010
Received in revised form
9 January 2011
Accepted 13 January 2011
Available online 21 January 2011

Keywords:
Danshen
Miltipolone
Inhibitory activity
Tautomeric effect
Metal ion chelator

ABSTRACT

Miltipolone (**1**) was discovered as a good and broad-spectrum inhibitor against the growth of cancer cells from "Danshen" based on the activity-driven screening of TCMs. The structural features make **1** easily tautomerize between different forms and **1** is linked and stabilized by intermolecular O–H···O hydrogen bonds in the crystal structure. The interaction of **1** in ddH_2O solution with Co^{2+}, Mn^{2+}, Zn^{2+}, Fe^{2+} or Fe^{3+} changed UV absorption values; the chelation of **1** with Fe^{2+} or Fe^{3+} also altered the characteristic UV absorption peaks. However, only did Fe^{2+} reverse **1**'s inhibition against the growth of cancer cells; therefore, we concluded that **1** possibly acts as a Fe^{2+} chelator to conduct its inhibitory activity.

1. Introduction

"Danshen", the dried root of *Salvia miltiorrhiza* Bunge (Labiatae) and one of the most widely used traditional Chinese Medicines (TCMs), has been used for treatment of heart stroke, angina pectoris and myocardial infarction [1–4] for a very long time. In recent years, "Danshen" is also used as antioxidants [5] and antitumor agents [6,7] for cancer treatment. The major lipophilic constituents of this species are abietane-type diterpene pigments, which exhibit various biological and pharmaceutical interesting activities [5–8], such as cytotoxicity, antitumor, antioxidation and anti-inflammation.

Miltipolone (**1**, Fig. 1), a diterpenoid tropolone, was first isolated from "Danshen" by Kakisawa and colleagues [9]. **1** showed excellent cytotoxic activity against B16F10 (murine melanoma cell) and HCT-116 (human colon carcinoma). In a part of our studies on the activity-driven screening of active compounds against the growth of cancer cells from the Traditional Chinese Medicines (TCMs), **1** was rediscovered by us from "Danshen". In this report, we describe identification of **1** and **1**'s broad-spectrum growth inhibitory activity to cancer cells. We show herein the tautomeric properties, the crystal structure and metal ion chelating functions of **1**. It was found that only did Fe^{2+} reverse **1**'s inhibition against the growth of cancer cells; therefore, we concluded that **1** possibly acts as a Fe^{2+} chelator to conduct its inhibitory activity.

2. Results and discussion

2.1. Identification of miltipolone (*1*) from "Danshen" and its broad activities against cancer cell lines

Based on the activity-driven screening of anticancer compounds from "Danshen", pure compound of miltipolone (**1**) was purified from the active fraction (ZP-14-PEA-ZXA-4a, Supplementary data Figs. s2c and s2d), which was as colorless prisms with a molecular formula of $C_{19}H_{24}O_3$ (HR FABMS: *m/z* 301.1793 $[M+1]^+$, calcd. for $C_{19}H_{25}O_3$, 301.1798). The structure of **1** was characterized by spectroscopic methods and identified by comparison to reported data [9] of MS, ^1H NMR and ^{13}C NMR spectra (see Supplementary data Figs. s3 and s4).

* Corresponding author. Guangzhou Institute of Biomedicine and Health, Chinese Academy of Sciences, Guangzhou, Guangdong 510530, PR China. Tel.: +86 013433968219; fax: +86 20 32015351.
E-mail address: allspringzhou@yahoo.com (G.-C. Zhou).
[1] Present address: Institute of Materia Medica, Chinese Academy of Medical Sciences and Peking Union Medical College, Beijing 100050, PR China.

0223-5234/$ – see front matter © 2011 Elsevier Masson SAS. All rights reserved.
doi:10.1016/j.ejmech.2011.01.026

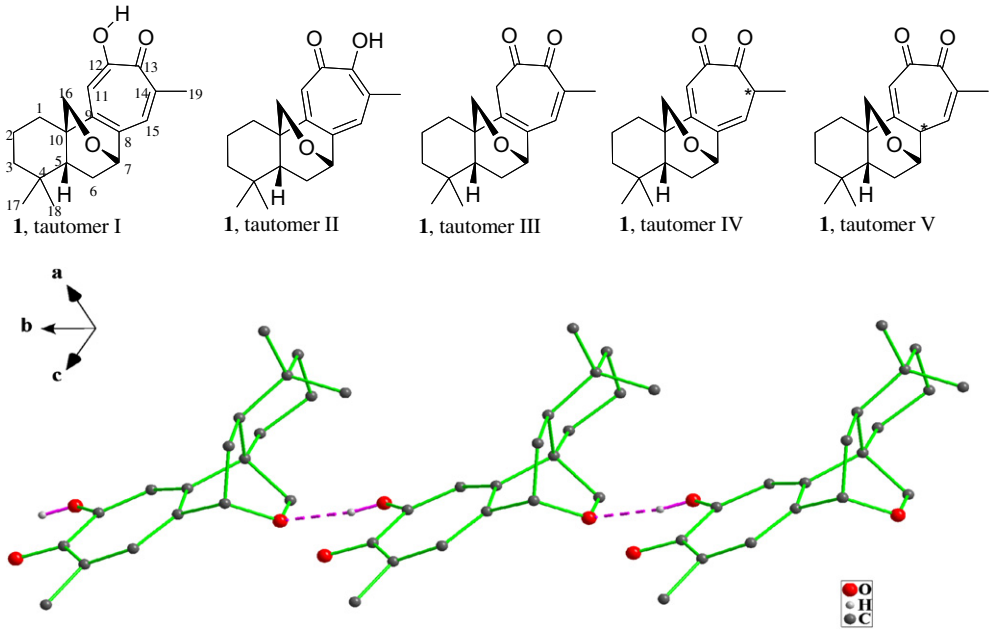

Fig. 1. The tautomeric structures (upper) and the crystal structure (lower) of miltipolone (**1**). Upper: possible tautomers of miltipolone (**1**) (asterisks represent stereo-centers); Lower: the cyclohexene (C7/C8/C9/C10/C5/C6) and cyclohexane (C2/C1/C10/C5/C4/C3) in **1** adopt boat conformation and chair conformation, respectively. The molecules of **1** are linked by intermolecular O–H···O hydrogen bonds into a chain parallel to the b axis and the crystal structure is stabilized by intermolecular O–H···O hydrogen bonds.

With pure **1** in hand, we expanded its inhibitory activity to other cancer cell lines (see Supplementary data Table s1). As shown in Table 1, **1** is a broad-spectrum cancer cell growth inhibitor that exhibited good activities against all of 10 tested cancer cell lines in our laboratory with IC_{50} range from 6.00 to 0.90 μM, meanwhile, **1** showed relatively weak activity against human umbilical vein endothelial cell (HUVEC) proliferation.

2.2. Structural properties of miltipolone (*1*)

It is anticipated that the structural characteristics bring **1** easily to tautomerize between enol and ketone forms and to produce 5 possible tautomers (Fig. 1). Since two tautomers (tautomers IV and V in Fig. 1) have their distinct chiral centers, **1** can generate up to 7 possible isomers in total. The specific isomer of **1** may exist in distinct circumstance and the NMR structure in $CDCl_3$ should be tautomer I or II (Fig. 1). The single crystal was grown in methanol at room temperature and the crystal structure of **1** was resolved by X-ray crystallography as tautomer I (CCDC 759536, Fig. 1 and page 9 of Supplementary data). The crystal structure showed that tautomer I of **1** was linked and stabilized by intermolecular O–H···O hydrogen bonds (Fig. 1) but not intramolecular O–H···O hydrogen bonds.

Table 1
IC_{50} values of miltipolone (**1**) against 10 cancer cell lines and HUVEC.

Cell type	Cell	IC_{50} (μM)
Endothelial cell	HUVEC	~20.0
Human lung cancer	A549	1.92 ± 0.15
Human liver cancer	Bel–7402	0.90 ± 0.06
	Hep G2	2.00 ± 0.13
Human cervical cancer	Hela	1.44 ± 0.13
Human breast cancer	MCF-7	2.00 ± 0.46
Human leukemia	Jurkat	1.40 ± 0.16
Human fibrosarcoma	HT1080	1.36 ± 0.41
Human melanoma	A375	3.50 ± 0.18
Human gastric carcinoma	NCI-N87	1.60 ± 0.05
Human pancreatic carcinoma	PANC-1	5.95 ± 0.34

1 showed single peak by normal phase HPLC analysis (Supplementary data Fig. s5). In order to demonstrate that **1** can exist in different isomers, we tested the effects of the acidic and basic conditions on the tautomeric equilibriums between the enol and ketone forms. Pure **1** was dissolved in ethanol, 50% ethanol-50% ddH_2O (double distilled water) or 50% ethanol-50% 0.2 M phosphate buffer (pH 4.5 with 0.22 M K^+, pH 5.9 with 0.22 M K^+, pH 7.0 with 0.32 M K^+ or pH 8.0 with 0.38 M K^+) to establish their respective original forms and then these solutions were analyzed by reverse phase HPLC using different pH eluents. As shown in Fig. 2a, **1** exhibited a sharp single peak eluting with acidic eluents (1% HOAc) (Fig. 2a) regardless of their original solutions, indicating that the acidic condition of 1% HOAc made **1** rapidly equilibrate from original tautomeric forms. However, single peak or partly overlapped multiple peaks with different retention times under neutral (ddH_2O) (Fig. 2b) and basic (0.02 M phosphate buffer with 0.038 M K^+, pH 8.3) (Fig. 2c) elution conditions were observed for different solutions, suggesting that the peak/s might be corresponding to one or some of these seven tautomers and original tautomers did not equilibrate fast enough in reverse HPLC under these pH or/and K^+ conditions.

2.3. Chelation of miltipolone (*1*) with metal ions in ddH_2O solution

The structural features of **1** attracted us to postulate that **1** is a metal ion chelator and its inhibitory activity to cancer cells is associated with one or some ions. To examine this hypothesis, we studied the interaction of **1** with physiologically important ions in ddH_2O solution. Even metal ions of Ca^{2+}, Mg^{2+}, K^+, Na^+, Fe^{2+}, Fe^{3+}, Zn^{2+}, Co^{2+} and Mn^{2+} are essential for physiological activities, the last 5 metal ions of Fe^{2+}, Fe^{3+}, Zn^{2+}, Co^{2+} and Mn^{2+} were considered for the interaction with **1** in our studies since the concentrations of Ca^{2+}, Mg^{2+}, K^+ and Na^+ in cell media of RPMI-1640 and DMEM are much higher than that of **1** applied in cell culture. Low concentration (0.25 μM) of Fe^{3+} is included in DMEM medium and not in RPMI-1640 medium and other 4 ions are not included in both media but all of these 5 ions should exist in the serum (NBCS or FBS) with limited quantity.

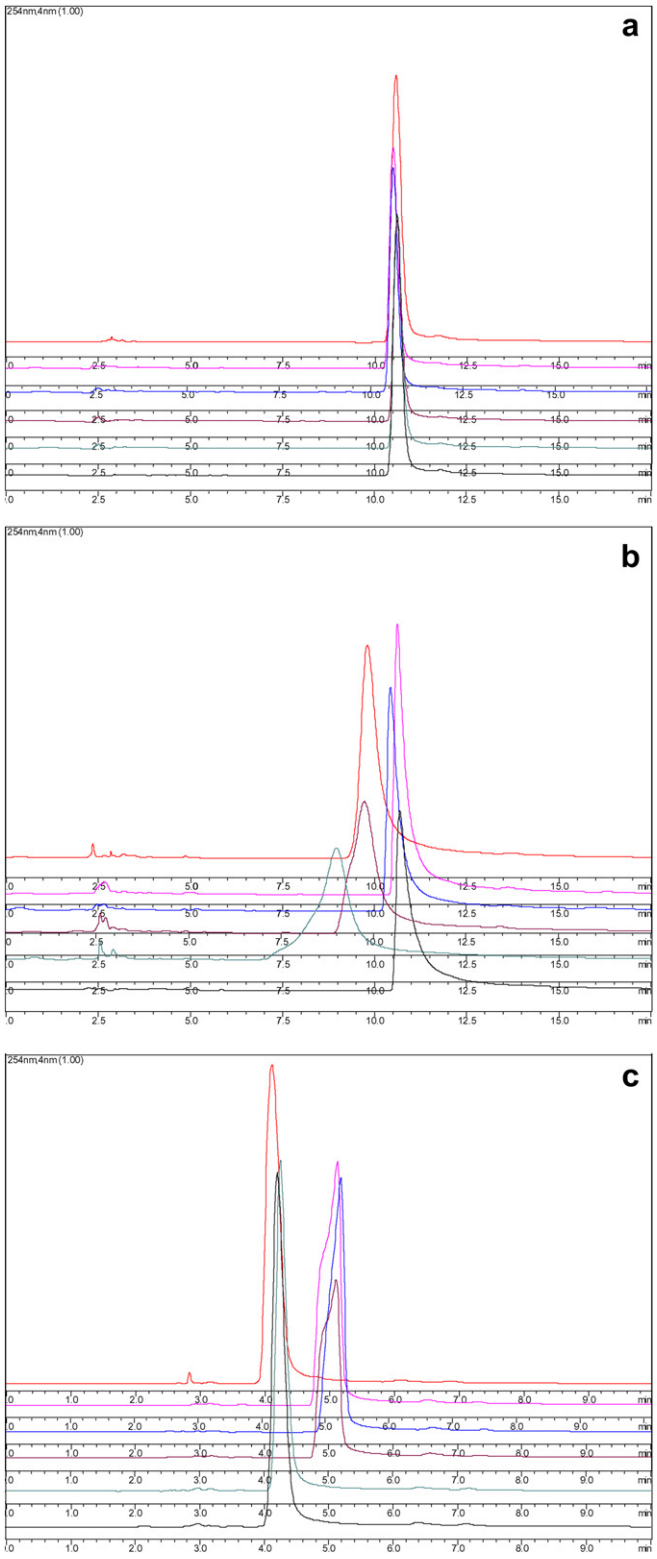

Fig. 2. Reverse phase HPLC analysis of pure 1 detected at 254 nm. Column: Diamonsil C18, 5.0 μm, 4.6 × 250 mm (Dikma Technologies); elution rate: 1.0 ml/min; loading quantity: 0.4 mg/ml × 20 μl; **1** was dissolved in 100% EtOH (red), 50% EtOH-50% 0.2 M phosphate buffer (0.22 M K^+, pH 4.5) (pink), 50% EtOH-50% 0.2 M phosphate buffer (0.22 M K^+, pH 5.9) (blue), 50% EtOH-50% 0.2 M phosphate buffer (0.32 M K^+, pH 7.0) (purple), 50% EtOH-50% 0.2 M phosphate buffer (0.38 M K^+, pH 8.0) (cyan) and 50% EtOH-50% ddH_2O (black). (a) elution by 80% MeOH with 20% (1% HOAc). (b) elution by 80% MeOH with 20% ddH_2O. (c) elution by 80% MeOH with 20% phosphate buffer (0.02 M phosphate buffer with 0.038 M K^+, pH 8.3). Preparation of buffers was listed in Supporting Information (page 11). (For interpretation of the references to colour in this figure legend, the reader is referred to the web version of this article.)

First, we explored the interaction of **1** with 5 physiologically important ions of Co^{2+}, Fe^{2+}, Fe^{3+}, Mn^{2+} and Zn^{2+} in ddH_2O solution containing 0.2% DMSO. In addition to make UV/Vis absorption intensity altered, the complex of **1** with Fe^{2+} shifted the characteristic UV absorption peak from ~244 nm to ~260 nm. The interaction of **1** with Fe^{3+} significantly changed UV/Vis absorption intensity and made absorption spectra from 300 to 380 nm changed but the contour of the characteristic UV absorption around 244 nm did not change (Fig. 3b). The addition of Co^{2+}, Mn^{2+} or Zn^{2+} into **1** changed UV/Vis absorption intensity, whereas, absorption spectra of the complexes were very similar to that of **1** (Supplementary data Fig. s6). These observations suggested that **1** is a strong chelator to Fe^{2+} and maybe also to Fe^{3+} but a relatively weak chelator to Co^{2+}, Mn^{2+} or Zn^{2+}.

It was shown in Fig. 3 that there are strong enough UV/Vis absorption of the complex of **1** with Fe^{2+} or Fe^{3+} from 400 to 470 nm, however, the absorption of **1** is steady in the baseline when $\lambda \geq 400$ nm. To know complex ratio between **1** and Fe^{2+} or Fe^{3+}, we titrated **1** with Fe^{2+} or Fe^{3+} and observed ion-dependent UV/Vis absorption relationships at two wavelengths (λ) of 425 and 450 nm. As shown in Fig. 3 insets, a linear increment manner continued until approximately 0.5 M equiv. of Fe^{2+} or Fe^{3+} was added, after which point, more quantity of Fe^{2+} and Fe^{3+} had little effect on the UV/Vis absorption. Therefore, it is proposed that the optimal complex ratios of **1** to Fe^{2+} and Fe^{3+} are 2.0 in ddH_2O solution.

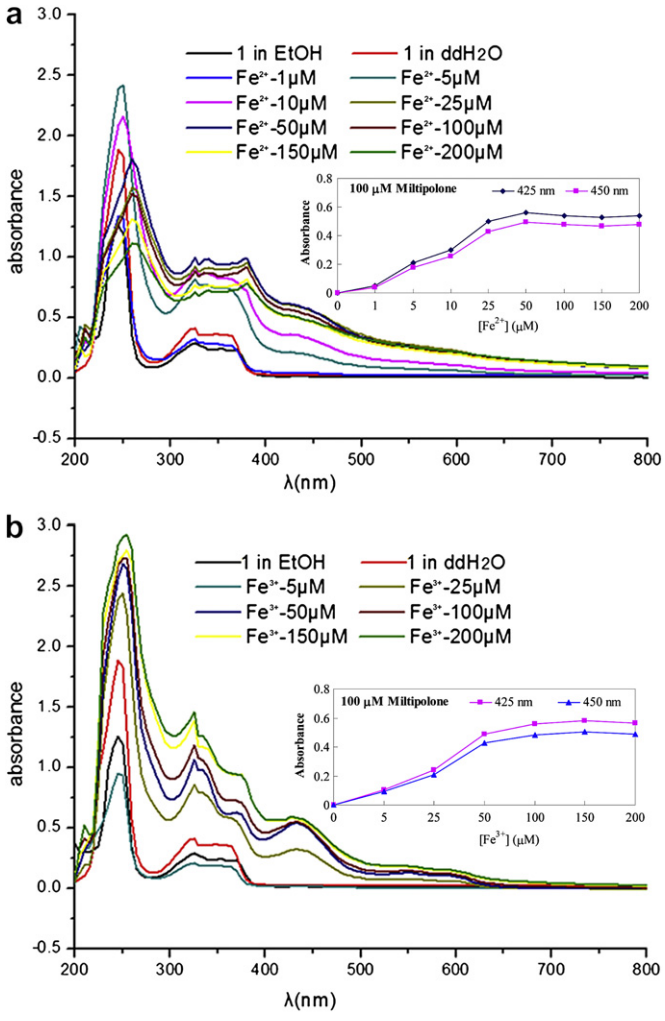

Fig. 3. UV/Vis spectra and chelating modes (insets) of **1** with (a) Fe^{2+} and (b) Fe^{3+}.

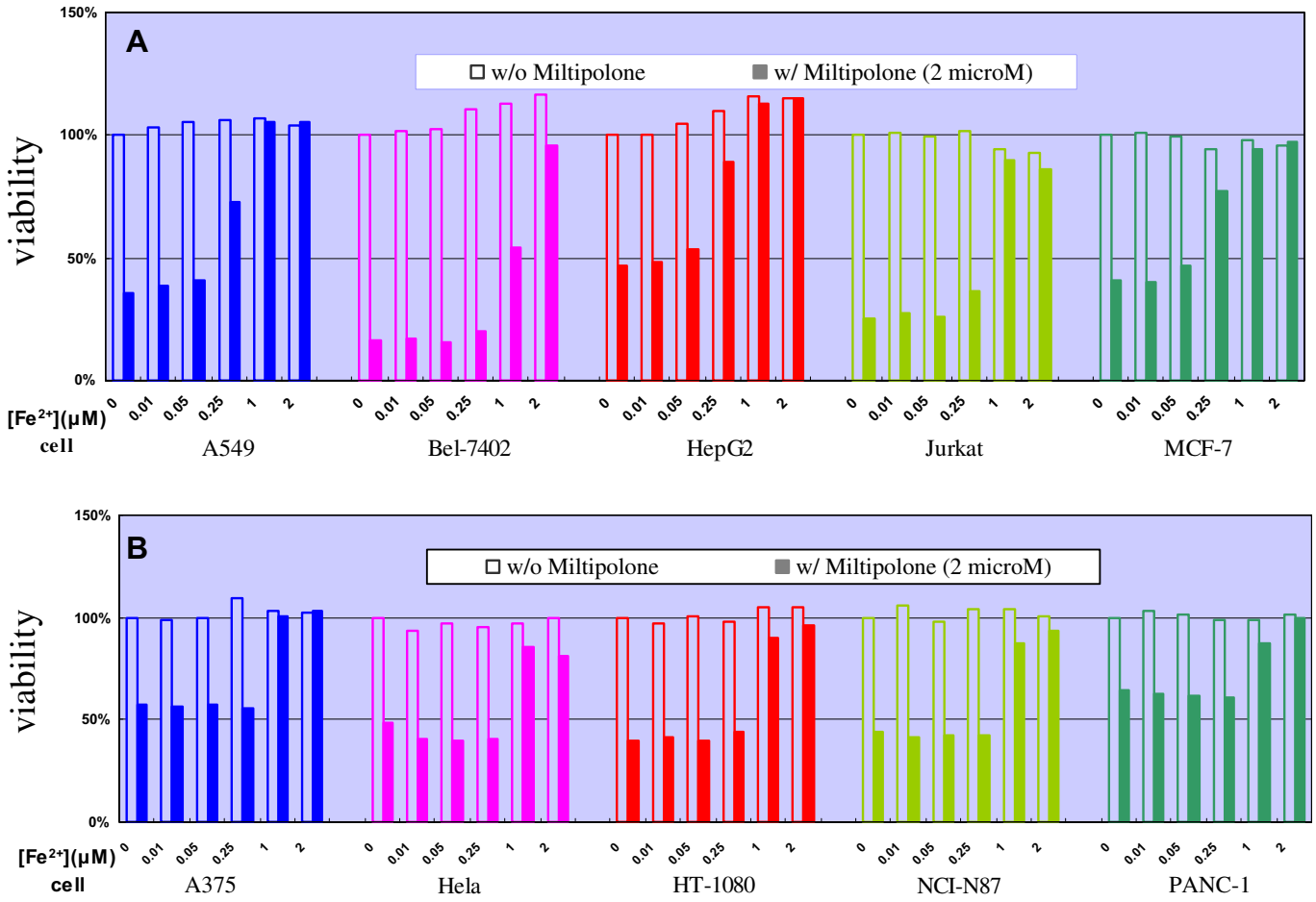

Fig. 4. Effects of Fe^{2+} on growth inhibition by 2.0 μM of **1**. (a), A549, Bel-7402, Hep G2, Jurkat and MCF-7; (b), A375, Hela, HT1080, NCI-N87 and PANC-1.

*2.4. Effects of ions on cancer cell growth inhibition by miltipolone (**1**)*

After we understood the interaction of **1** with these ions in ddH_2O solution (Fig. 3), we next were interested in investigating if the interaction is associated with **1**'s activities against cancer cells in cell culture. All of 10 cancer cell lines in Table 1 were used as target cells and the final concentration of **1** was fixed at 2.0 μM, at which inhibition rate without metal ions was close or more than 50%. Then, the cells were titrated with different concentrations of 5 ions. The experimental data demonstrated that Fe^{2+} reversed the growth inhibition by **1** to these cancer cell lines and the cell viability was dependent on Fe^{2+} concentration (Fig. 4); however, Fe^{3+} and other 3 ions did not show antagonistic effect on **1** against cell growth of 10 cancer cell lines (Supplementary data Fig. s6). In addition, the inhibitory activities of **1** to cancer cells except Bel-7402 were almost fully reversed when the concentration of Fe^{2+} reached 1.0 μM. These facts suggested that the optimal complex ratio of **1** to Fe^{2+} is 2.0 in both of ddH_2O solution and cell cultures. Therefore, we concluded that the action of **1** against the proliferation of cancer cells is possibly mediated by Fe^{2+} ion even both of Fe^{2+} and Fe^{3+} can strongly interact with **1** in ddH_2O solution. Because of these, it is speculated that the structural moiety contributed for characteristic UV absorption around 250 nm is more important for **1**'s inhibitory activity than the structural features represented for UV spectra from 300 to 380 nm. This information will give us a helpful clue in future anticancer drug design based on **1**.

3. Conclusions

In summary, miltipolone (**1**) was rediscovered based on the activity-driven screening from "Danshen" and **1** is a good and broad-spectrum growth inhibitor to cancer cells. The crystal structure of **1** suggests that the formation of intermolecular hydrogen bond is superior to that of intramolecular hydrogen bond in crystal state. It is anticipated that the structural features of **1** lead to its tautomerization and can generate up to 7 possible isomers. **1** in ddH_2O solution acts as a strong chelator to Fe^{2+} and Fe^{3+}, however, only did Fe^{2+} reverse the growth inhibition of all 10 cancer cell lines by **1**. It was demonstrated that the optimal complex ratio of **1** to Fe^{2+} is 2.0 in both of ddH_2O solution and cell cultures. Our current data suggested that the structural moiety contributed for UV absorption around 250 nm is more important for **1**'s inhibitory activity than the structural features represented for UV spectra from 300 to 380 nm. This information provides a basis for anticancer drug design using **1** as a lead compound. Further studies on elucidation of binding target/s and detailed action mechanism/s of **1** are under way.

4. Experimental

4.1. General experimental information

^{1}H and ^{13}C-NMR spectra were recorded on a Bruker AV-400 spectrometer at 400 and 100 MHz, respectively, in $CDCl_3$. The high resolution FABMS was recorded on a Thermo MAT 95XP mass spectrometer.

Samples were dissolved in methanol or ethanol for reverse phase HPLC and in ethyl acetate for normal phase HPLC. Analytic HPLC was performed on DIONEX SUMMIT HPLC with PDA-100 Photodiode Array Detector or Shimadzu LC-20AT with SPD-M20A Diode array detector, and preparative HPLC was conducted by Shimadzu 14A with UV detector set at 254 and 280 nm. Analytic columns were Diamonsil C18 (5.0 μm, 4.6 × 250 mm, Dikma Technologies) for reverse phase HPLC and Venusil XBP-Si (5.0 μm, 100 Å, 4.6 × 150 mm, Agela Technologies Inc.) for normal phase HPLC, respectively. Preparative column for normal phase HPLC was Sepax HP-silica (10.0 × 250 mm, 5.0 μm, 120 Å, Sepax Technologies Inc.). More information was detailed in Supplementary data Fig. 2, s1, s2 and s5.

Human umbilical vein endothelial cells (HUVECs) were isolated from freshly delivered umbilical cords; all cancer cell lines were from ATCC; FBS (Fetal Bovine Serum) was obtained from Hyclone; NBCS (Newborn Calf Serum) was purchased from GIBCO; EGM-2 was from LONZA; RPMI 1640 and DMEM (Dulbecco's Modified Eagle's Medium) were bought from Hyclone. All cells were incubated at 37 °C and 5% CO_2. The information of cell lines, media, sera, positive compounds and cell numbers seeded for assays is summarized in Supplementary data Table s1.

4.2. Identification of miltipolone (**1**) by the activity-driven screening of anticancer active compounds from "Danshen"

The principle of the activity-driven screening from TCMs is that effective extraction and isolation of active fractions and purification of active constituents were conducted on the basis of the activity indications. Briefly, cancer cell lines A549 (human non-small cell lung cancer) and Bel-7402 (human hepatocarcinoma) were used as primary target cells. The active petroleum ether extracts (marked as ZP-14-PEA, $IC_{50} < 20$ μg/ml against several human cancer lines) of sliced roots of *S. miltiorrhiza* were separated into 6 fractions by normal phase HPLC using Sepax HP-silica column (10.0 × 250 mm, 5.0 μm) (see Supplementary data Figs. s1a and s1b). The 4th fraction (marked as ZP-14-PEA-ZX-4) showed the best activity against A549 and Bel-7402 with IC_{50} values (Supplementary data Figs. s1c and s1d) of 1.40 μg/ml and 0.50 μg/ml, respectively. The 4th fraction (ZP-14-PEA-ZX-4) was further separated into 3 fractions by normal phase HPLC using the same column as above (see Supplementary data Figs. s2a and s2b). The 2nd one (marked as ZP-14-PEA-ZXA-4a) among three fractions possessed the highest inhibitory activity (IC_{50}: 0.33 μg/ml to A549 and 0.27 μg/ml to Bel-7402, respectively. Supplementary data Figs. s2c and s2d). At the end, exhaustive purification by normal phase HPLC from the 2nd fraction (ZP-14-PEA-ZXA-4a) yielded pure compound of miltipolone (**1**) as colorless prisms, HR FABMS: *m/z* 301.1793 $[M + 1]^+$, calcd. for $C_{19}H_{25}O_3$, 301.1798. The structure of **1** was characterized by spectroscopic methods and identified by comparison to reported data [9] of MS, ^1H NMR and ^{13}C NMR spectra (see Supplementary data Figs. s3 and s4).

4.3. Antiproliferative activity assay

Miltipolone (**1**) was dissolved in DMSO and diluted by PBS into the stock solution containing 2% DMSO before use. The stock solution of carrier is 2% DMSO in PBS. The final concentration of DMSO is 0.1% for all wells. The activities of miltipolone (**1**) against the proliferation of 10 cancer cell lines and HUVEC were assayed by MTT method. Briefly, cells in 190 μl corresponding medium were seeded in 96-well plates and allowed to attach or stabilize for 20 h before treated with 10 μl stock solutions of different concentrations of **1** or carrier. Every concentration of **1** or carrier is in triplicate. After incubated for 96 h, cells were treated with MTT reagents and relative cell viability of each well was calculated. IC_{50} value of **1** was calculated based on the relationship of cell viability *vs* the corresponding concentration.

4.4. Ion-dependent UV/Vis absorption

UV/Vis absorption spectra were recorded using a Lambda 35 UV/Vis spectrometer (PerkinElmer) with a 1 cm path length. The 50.0 mM DMSO solution of **1** was diluted by ddH_2O into 1.0 mM stock solution of **1**. The detected solutions, which were 100 μM of **1** with 1, 5, 10, 25, 50, 100, 150 and 200 μM of $FeCl_2$, 5, 25, 50, 100, 150 and 200 μM of $Fe(NO_3)_3$ or 50, 100 and 200 μM of $CoCl_2$, $MnSO_4$ or $ZnCl_2$, were prepared by the addition of one part of 1.0 mM stock solution of **1** to 9 parts of different stock solution of the designated ion. The final concentration of DMSO was 0.2% and the absorbance of 0.2% DMSO solution without **1** was set to zero for all experiments. Scanning was conducted with 2 nm slit in a 50 μl quartz cuvette from 200 nm to 800 nm. The relationship of UV absorbance values with stepwise increased concentrations of $FeCl_2$ or $Fe(NO_3)_3$ was studied for chelating modes. Absorbance value was recorded at the wavelength of 425 or 450 nm in a 50 μl quartz cuvette and the net value was got after the background absorption of **1** at the same wavelength was subtracted.

4.5. Effects of ions on growth inhibition of 10 cancer cell lines by 2.0 μM of **1**

The 2.0 mM DMSO solution of miltipolone (**1**) was diluted by PBS into 40 μM of the stock solution containing 2% DMSO before use. The stock solution of carrier is 2% DMSO in PBS. Cancer cells in 180 μl corresponding medium were seeded in 96-well plates and allowed to attach or stabilize for 20 h before treated with 10 μl of the stock solution of **1** or carrier, and then 10 μl of gradient concentrations of an ion in ddH_2O or the same volume of ddH_2O. The media without **1** were used for the control wells while the media containing 2.0 μM of **1** were used for other wells. The final concentration of DMSO is 0.1% for all wells. Every experiment was in triplicate. After incubated for 96 h, cells were treated with MTT reagents and relative cell viability of each well was calculated on the basis of its corresponding control well.

Acknowledgements

We are pleased to acknowledge financial supports provided by the Teacher's Promotion Program of College of Sciences, Nanjing Agricultural University to J. Wang and the Knowledge Innovation Program of the Chinese Academy of Sciences (KSCX-2-YW-R-22) to G.-C. Zhou.

Appendix. Supplementary data

Supplementary data associated with this article can be found in the on-line version, at doi:10.1016/j.ejmech.2011.01.026.

References

[1] B. Wu, M. Liu, S. Zhang, Cochrane Database Syst. Rev. 4 (2004) [CD004295].
[2] C.S. Shi, H.C. Huang, H.L. Wu, C.H. Kuo, B.I. Chang, M.S. Shiao, G.Y. Shi, Thromb. Res. 119 (2007) 769–775.
[3] X.Y. Ji, B.K. Tan, Y.Z. Zhu, Acta Pharmacol. Sin. 21 (2000) 1089–1094.
[4] J.D. Adams, R. Wang, J. Yang, E.J. Lien, Chin. Med. 1 (2006) 3.
[5] W.L. Wu, W.L. Chang, C.F. Chen, Am. J. Chin. Med. 19 (1991) 207–216.
[6] S.Y. Ryu, C.O. Lee, S.U. Choi, Planta Med 63 (1997) 339–342.
[7] X. Wang, K.F. Bastow, C.M. Sun, Y.L. Lin, H.J. Yu, M.J. Don, T.S. Wu, S. Nakamura, K.H. Lee, J. Med. Chem. 47 (2004) 5816–5819.
[8] D.Y. Kong, Chin. J. Pharm. 20 (1989) 279–285.
[9] G. Haro, M. Mori, M.O. Ishitsuka, T. Kusumi, Y. Inouye, H. Kakisawa, Bull. Chem. Soc. Jpn. 64 (1991) 3422–3426.